3rd IAHR International Meeting of the Workgroup on Cavitation and Dynamic Problems in Hydraulic Machinery and Systems, October 14-16, 2009, Brno, Czech Republic

3D NUMERICAL ANALYSIS OF THE UNSTEADY TURBULENT SWIRLING FLOW IN A CONICAL DIFFUSER USING FLUENT AND OPENFOAM

Sebastian MUNTEAN*

Centre for Advanced Research in Engineering Sciences, Romanian Academy – Timisoara Branch, Romania

Håkan NILSSON

Department of Applied Mechanics, Chalmers University of Technology, Sweden

Romeo F. SUSAN-RESIGA

Hydraulic Machinery Department, Politehnica University of Timisoara, Romania

ABSTRACT

The paper presents three-dimensional numerical investigations of the unsteady swirling flow in a conical diffuser with a precessing vortex rope. The helical vortex breakdown, also known as precessing vortex rope in the engineering literature, benefits from a large body of literature aimed either at elucidating the physics of the phenomenon and building mathematical models, or at developing and testing practical solutions to control the causes and/or the effects. In this paper we investigate the unsteady hydrodynamic fields with a well-known precessing vortex rope computed with the FLUENT and OpenFOAM CFD codes. The main goal is to elucidate the physics of the phenomenon. The three-dimensional computational domain corresponds to the test section of a test rig designed and developed at Politehnica University of Timisoara. The same domain and grid with two millions cells is considered in both codes. The boundary conditions and problem setup are presented for each case. The unsteady pressure fluctuations along to the element of the conical diffuser are recorded. The numerical pressure fluctuations are validated against experimental data measured on the wall of the test rig. Consequently, the fundamental frequency and higher harmonics of the vortex rope is determined by a Fourier analysis.

KEYWORDS

unsteady turbulent swirling flow, conical diffuser, precessing vortex rope, numerical simulation

1. INTRODUCTION

The paper presents numerical investigations of swirling flow with a precessing vortex rope in a conical diffuser, and its associated pressure fluctuations. Consequently, the main goal of this paper is to investigate numerically the flow in a straight draft tube, for a better understanding of the 3D swirling flow physics as well as how the pressure fluctuations are associated to the precessing vortex rope. The helical vortex breakdown, also known as

* *Corresponding author:* Center for Advanced Research in Engineering Sciences, Romanian Academy – Timisoara Branch, Bv. Mihai Viteazu 24, Timisoara, Romania, phone: +40256403692, fax: +40256403692, email: seby@acad-tim.tm.edu.ro

precessing vortex rope in the engineering literature, benefits from a large body of literature aimed either at elucidating the physics of the phenomenon, and building mathematical models or at developing and testing practical solutions to control the causes and/or the effects. The decelerated swirling flow often results in vortex breakdown above a certain level of the swirl number [1]. This vortex breakdown is now recognized as the main cause of the severe pressure fluctuations experienced by hydraulic turbines operating at part load. The pressure fluctuations are caused by the transformation of an axis-symmetrically swirling flow into one or more precessing helical vortices as the operating condition shifts towards part load. The precessing motion of the helical vortex results in a fluctuating pressure on any stationary point of the draft tube cone. In addition, a limited quantity of air or water vapor in the flow provides a degree of elasticity, termed cavitation compliance, and this elasticity can lead to a form of resonance in the draft tube excited by the precessing inhomogeneous pressure field associated with the spiral vortex core [2].

The self-induced unsteadiness of swirling flow downstream Francis turbine runners at part load has been associated with possible severe flow separation on the blade's suction side. However, the swirling airflow experiments of Cassidy and Falvey [3] aimed at establishing guidelines for the surge characteristics of hydraulic turbines showed that the spiral vortex breakdown is responsible for the flow unsteadiness. They showed that above a critical swirl number, both the Strouhal number and the pressure amplitude were linearly dependent on the swirl number. A similar radial guide vane apparatus has been used by Nishi et al. [4] to investigate the water swirling flow in a 9.5^{o} conical diffuser. The periodic flow field has been measured with a five-hole probe system. They showed that the dimensionless peak-to-peak pressure fluctuation and the corresponding dimensionless fundamental frequency are constant at high cavitation parameter values, but decrease monotonically as vortex cavitation develops. In addition, Nishi et al. [4] suggest that the circumferentially averaged velocity profiles in the cone could be represented satisfactorily by a model comprising a dead (quasi-stagnant) water region surrounded by the swirling main flow. This model is also supported by the measured averaged pressure, which remains practically constant within the quasi-stagnation region [5]. This result is also supported by the PIV investigation of the velocity field in the straight draft tube [6].

The main goal of the present paper is to investigate the decelerated swirling flow with a precessing vortex rope to better understand the physics of phenomena. First, the 3D computational domain and setup corresponding to the experimental test rig is depicted. Second, the numerical simulation setup and numerical results using the FLUENT and OpenFOAM CFD codes are presented. Next, the numerical result are validates against experimental data. Finally, considerations about swirling flow with a precessing vortex rope and further perspectives are outlined in the last section.

2. 3D COMPUTATIONAL DOMAIN AND BOUNDARY CONDITIONS

A meridian cross-section of the swirling flow apparatus [7] is shown in Fig. 1. The swirling flow apparatus includes a swirl generator and a convergent-divergent test section. The central body ensemble, called swirl generator, includes: leaned strouts, guide vanes, free runner and nozzle. The design of the tandem cascades is presented in [8], [9], [10]. The first row of blades, called guide vanes, produce a flow with practically constant total pressure. Consequently, constant axial velocity and a free vortex tangential velocity is obtained. The second row of blades, called free runner, has the main purpose of re-distributing the total pressure by inducing an excess near the shroud and a correspoding deficit near the hub. The runner blades act like a turbine near the hub, and like a pump near the shroud, with a vanishing total torque. As a result, the runner spins freely on the hub. This particular setup is

aimed at producing a swirling flow at the throat section, similar to the one encountered in Francis turbines operated at partial discharge, [11].

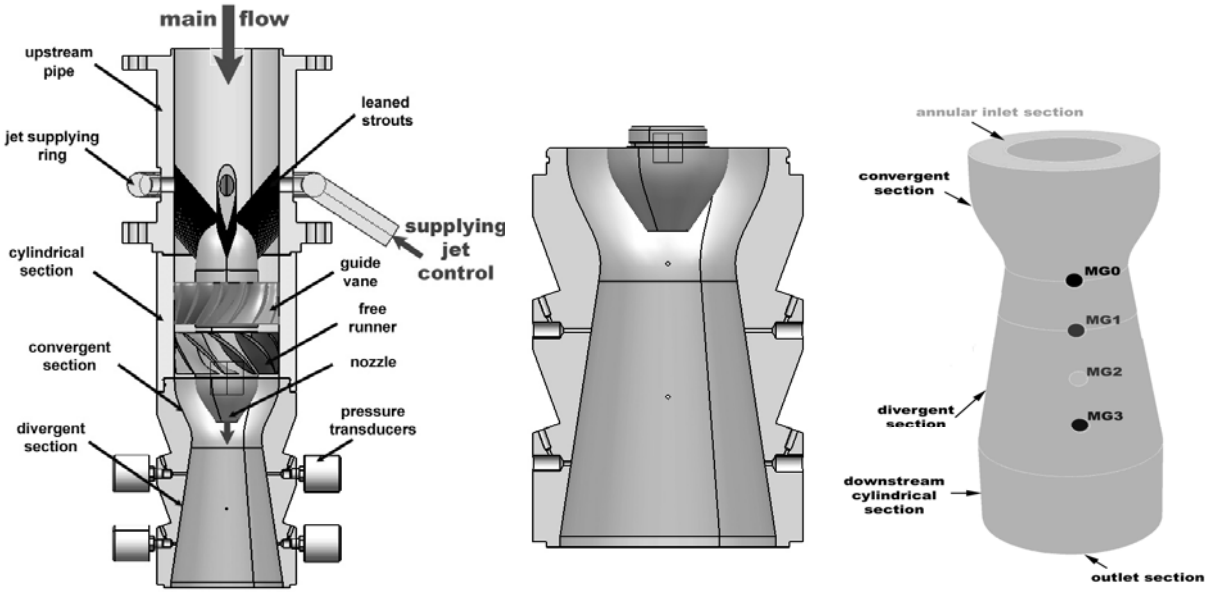

Fig. 1 Meridian cross-section of the swirling flow apparatus (left), zoom-up of the convergent-divergent test section (center) and 3D computational domain with pressure tap markers (right).

The throat diameter is 100 mm, with a nominal discharge of 30 l/s. The conical diffuser has a 8.5° half-angle and 200 mm in length. The design of the convergent-divergent test section is presented in Bosioc et al. [12], and it has been manufactured from plexiglass in order to allow flow visualization. The unsteady static pressure is measured at four positions (MG0, MG1, MG2 and MG3) along to the element of the cone. The sections are located 0, 50, 100 and 150 mm downstream the throat.

The 3D computational domain corresponds to the convergent-divergent section of the test rig. The inlet boundary of the computational domain is the annular section just downstream the free runner while the outlet section belongs to a cylindrical extension of the divergent part.

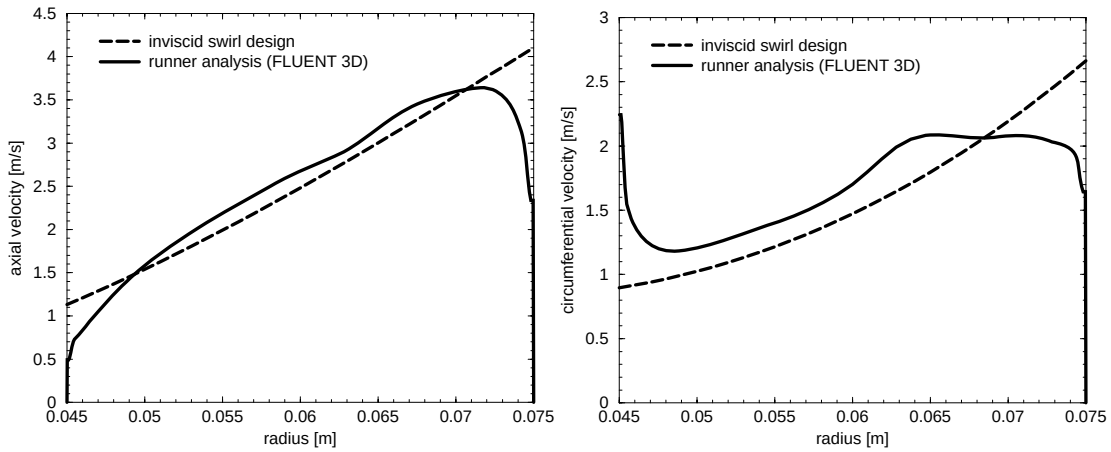

Fig. 2 Axial and circumferential velocity profiles imposed at the inlet of the 3D computational domain.

Fig. 2 shows the inviscid design of the swirl just downstream the runner (dashed lines) and the actual velocity profiles from a turbulent 3D numerical analysis of the flow in the runner. Although the axial velocity closely follows the intended profile, the circumferential velocity cannot reach the intended profile near the shroud. However, this 3D turbulent velocity profile is used as inflow condition in our numerical computations, together with profiles of turbulence kinetic energy and dissipation from the same numerical results.

3. EXPERIMENTAL DETAILS

The test rig developed at the UPT – NCESCF is designed to investigate different control techniques in order to mitigate precessing vortex rope generated in swirling flows [7]. Consequently, the test rig is equipped with an integrated data acquisition system in order to record the flow rates and the unsteady pressure up to 12 taps. Consequently, this system includes: a PC with NI board with 32 channel and LabVIEW software, SCB-68 terminal block, Cole-Parmer unsteady pressure transducers, flowmeters and wires. In this case, eight unsteady pressure transducers are flush mounted on the cone wall to four levels, see Fig. 3. The first level corresponds to the throat and the next levels are displaced at 50, 100 and 150 mm relative to the first one. The transducers measurement range was ±1 bar with a precision of ±0.13%. However, the upper limit of frequency for unsteady pressure transducers is around 50 Hz. In our experimental investigations of the swirling flows into the conical diffuser, the vortex breakdown evolves into precessing spiral vortex (vortex rope). In this paper only the non-cavitating vortex rope is investigated.

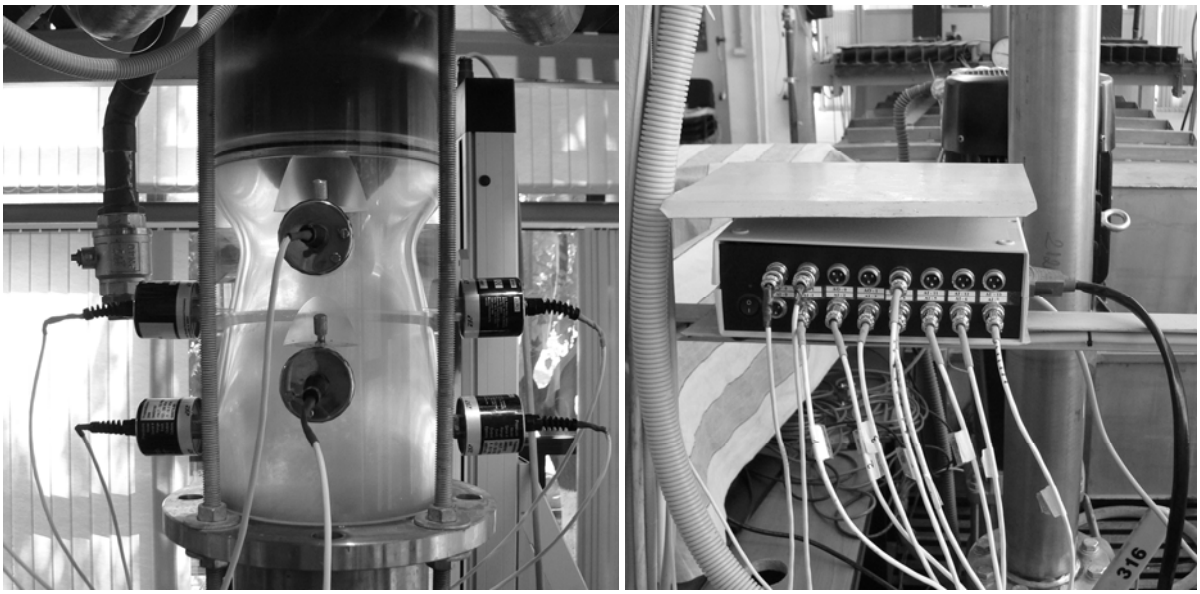

Fig. 3 The unsteady pressure transducers flush mounted on the test section and the integrated data acquisition system.

4. FLUENT AND OPENFOAM SET-UP

The simulations presented in this work were done with the FLUENT 6.3 and OpenFOAM-1.5.x CFD codes. FLUENT is a well-known commercial code, while OpenFOAM has been available as Open Source since the end of 2004. The OpenFOAM CFD toolbox (www.openfoam.org) has been described, used and validated for swirling flow in hydraulic turbine draft tubes [17], [18] and diffusers [19]. Both simultations use the same 3D computational mesh with two million cells [14], and both codes were run in parallel. Both simulations solve the unsteady Reynolds-averaged Navier-Stokes equations with a two-

equation turbulence model closure. The inlet boundary condition used for both codes is specified as described in section 2.

- **FLUENT specific set-up**: According to the FLUENT developers [15], both the RNG *k-ε* model and the realizable *k-ε* model yield appreciable improvements over the standard *k-ε* model for flows with weak to moderate swirl. Consequently, the realizable *k-ε* model is selected together with enhanced wall treatment and pressure gradient effects. The radial equilibrium condition was used at the outlet, based on previous validations [13]. The time step was 10^{-4}s.
- **OpenFOAM specific set-up**: A preliminary OpenFOAM simulation of the present case using therealizable *k-ε* model yielded a low-frequency axial fluctuation. The fluctuation correlated perfectly with the region of reversed flow periodically reaching the outlet. The same fluctuation was obtained in a computational domain with an extended outlet section, where there was no reversed flow at the outlet, so it seems like the realizable *k-ε* model in OpenFOAM resolves an additional flow feature. The low-frequency fluctuation correlated perfectly with the region of reversed flow periodically reaching the outlet. The standard k-ε model, on the other hand, yielded periodic results with respect to the vortex rope frequency, and there was never any reversed flow at the outlet. In this paper it is thus the standard k-ε results that represent the results from OpenFOAM. At the walls, a standard log-law wall treatment is applied. The average y+ values range between 40-240, except in the separated region below the central body, where it increases to 400, but in that region the log-law doesn't make sense anyway. The velocity and turbulence equations use the homogeneous Neumann boundary condition at the outlet. The pressure equation uses a homogeneous Neumann boundary at all boundaries, and at the outlet the mean pressure is set to zero. The convection terms are discretized using a 2nd order linear-upwind scheme, and the time terms are discretized using the 2nd order Crank-Nicholson scheme with a blending with the Euler implicit scheme for numerical stability. The time step is half that of the Fluent simulation, i.e. 5e-5, yielding a maximum Courant number of 0.91.

5. VISUALIZATION OF THE INSTANTANEOUS RESULTS

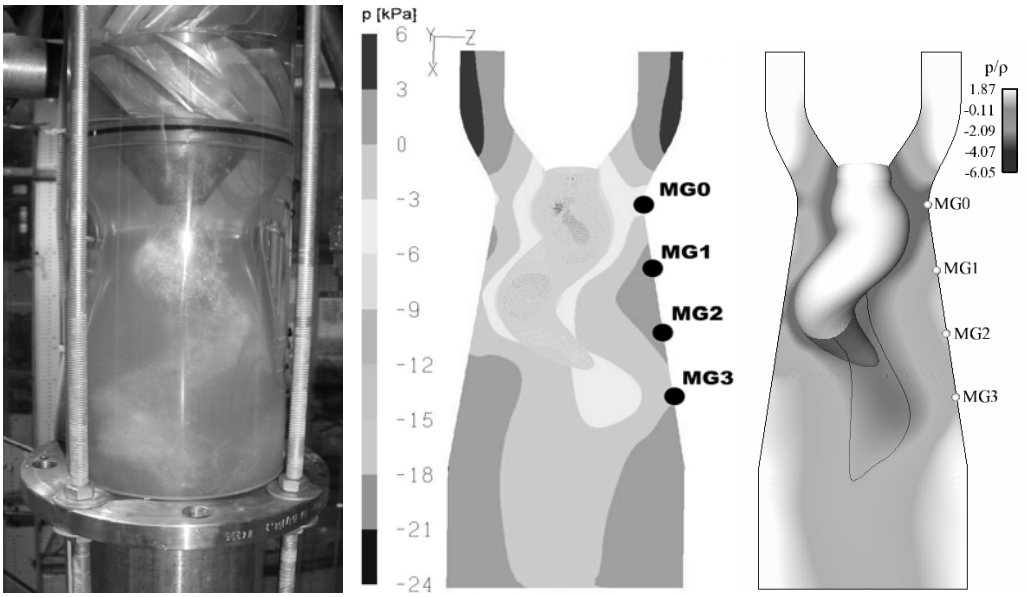

Fig. 4 The precessing vortex rope visualized in the experimental test section (left), and snap-shots from the FLUENT (center) and OpenFOAM (right) simulations. Note that the mean outlet static pressure is set to zero in the simulations.

Both simulations reproduce the well-known precessing vortex rope. The vortex rope is visualised in Fig. 4 using a snap-shot of an iso-surface of constant static pressure. The meridian cross-section is colored by the static pressure, and an iso-line of zero axial velocity visualizes the region of reversed flow. This three-dimensional precessing helical vortex induces an unsteady pressure field. Four numerical pressure monitors (MG0, MG1, MG2 and MG3) are located along to the element of the cone in the same locations as the pressure taps on the experimental setup, see Fig. 1.

6. FOURIER ANALYSIS OF THE PRESSURE FLUCTUATIONS

The recorded pressure fluctuations at locations MG0 - MG3 are examined using a Fourier analysis. Let f be a real periodic valued function of time with period T. Suppose we sample f at N equally spaced time intervals of length Δ seconds starting at time t_0. That is we have $s_i = f(t_0 + i\Delta),\ i = 0,1,...,N-1$. In particular, it assumes that $f(t_0) = f(t_0 + N\Delta)$. Hence, the period is assumed to be $T = N\Delta$. The interpolating trigonometric polynomial $g(t)$ which approximates the function $f(t)$, can be written as

$$g(t) = A_0 + \sum_{n=1}^{(N-1)/2} A_n \cos[\omega_n (t - t_0)] - \sum_{n=1}^{(N-1)/2} B_n \sin[\omega_n (t - t_0)] \tag{1}$$

where

$$A_0 = \frac{c_0}{N} = \frac{1}{N}\sum_{n=0}^{N-1} s_n\ ;\ A_{\mathrm{n}} = \frac{2c_{2\mathrm{n}}}{N}\ ;\ B_{\mathrm{n}} = \frac{2c_{2\mathrm{n}+1}}{N}\ ;\ \omega_{\mathrm{n}} = \frac{2\pi(n+1)}{N\Delta} = \frac{2\pi(n+1)}{T}$$

Obviously, A_0 is the average value of the samples, while the A_n and B_n coefficients are the cosine and sine modes amplitudes, respectively, for the angular frequency ω_n.

The FFTRF subroutine from International Math and Statistics Libraries (IMSL) [16] is used to compute the discrete Fourier transform and the reconstruction signal. The numerical unsteady pressure recorded in all monitors (MG0 – MG3), and reconstruction signals are plotted in Fig. 5, and the corresponding frequency spectra are plotted in Fig. 6. The Strouhal number can be computed from these results according to

$$St = \frac{f \cdot l}{V} = \frac{f \cdot D}{\left(\dfrac{4 \cdot Q}{\pi \cdot D^2}\right)} \tag{2}$$

where D=100 mm is the throat diameter, Q=30 l/s nominal discharge and f is the fundamental frequency (in this case the vortex rope frequency).

- **FLUENT simulation discussion**: The pressure fluctuation in the throat (MG0) is reconstructed using only two harmonics. Moreover, the fluctuation seems to be quasi-sinusoidal since the 2nd harmonic is negligible (the 2nd harmonic amplitude is one order less than the 1st harmonic amplitude, see Fig. 5). Consequently, we can state the vortex rope is compact. At MG1 the pressure fluctuation is rebuilt with four harmonics. The amplitude of the 1st harmonic in MG1 is twice larger than the same amplitude in MG0. However, the 2nd harmonic is more significant than that from MG0. In this case, the 2nd harmonic amplitude is four times less than the 1st harmonic amplitude while the 3rd and 4th harmonics are negligible. As a result, the vortex rope is well developed. The pressure fluctuation at MG2 is reconstructed with seven harmonics. In this section, the 1st harmonic amplitude at MG2 has the same value as the 1st harmonic at MG1. Nevertheless, the next four harmonics (from second to five) are significantly larger. At MG3 the pressure fluctuation is reconstructed with eight harmonics. The amplitudes of the first four harmonics are of the same order of magnitude. However, these values are four times less than the 1st harmonic at MG2. Actually, one can assess that the vortex

rope gets closer to the wall triggering higher order harmonics as we advance downstream into the cone. Moreover, in this region the vortex rope tail is assumed. The vortex rope frequency is 15.5 Hz, corresponding to a Strouhal number of 0.406.

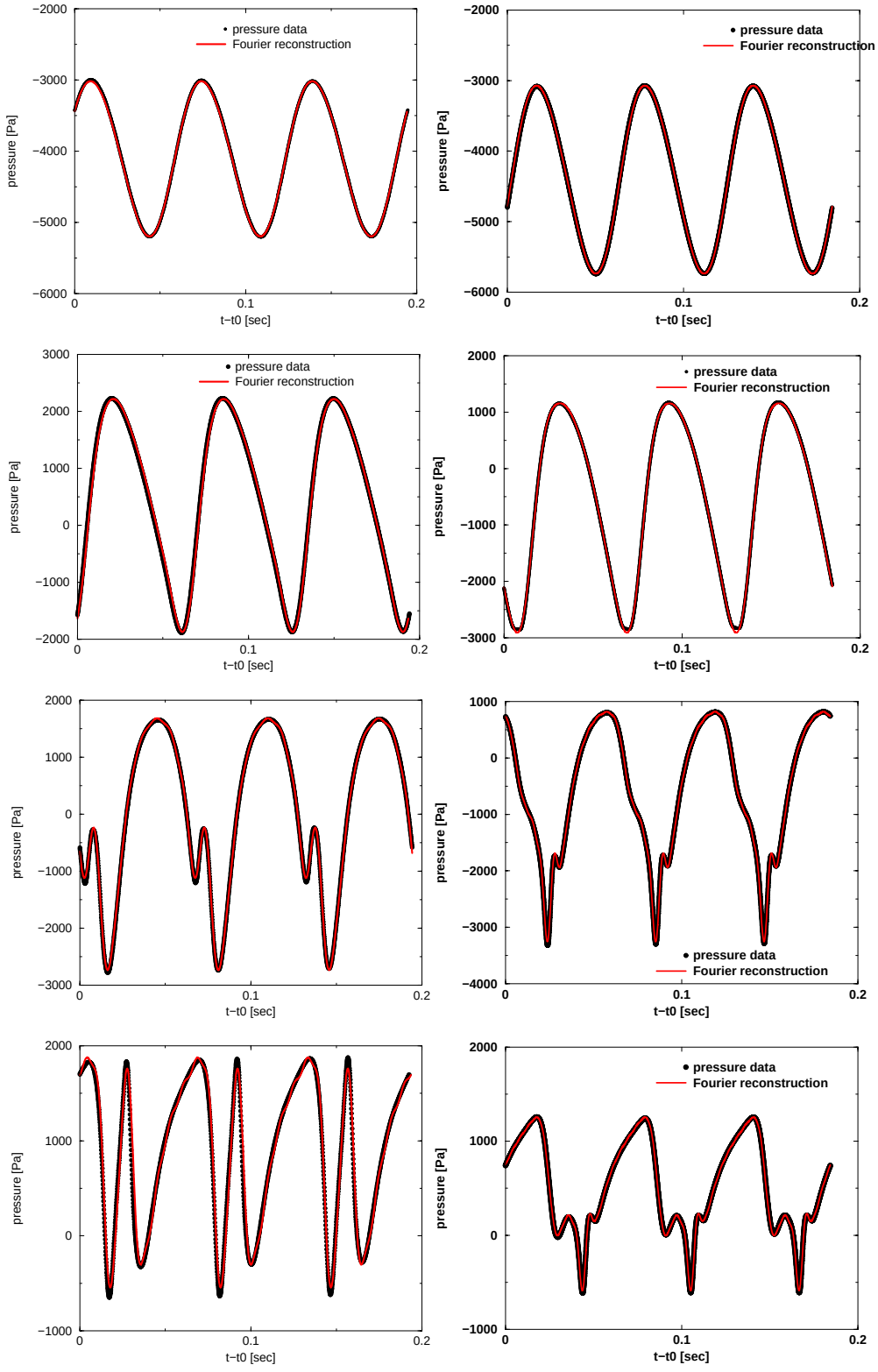

Fig. 5 Unsteady pressure recorded at MG0, MG1, MG2 and MG3(top to bottom) and Fourier reconstruction signal for FLUENT (left) and OpenFOAM (right).

- **OpenFOAM simulation discussion**: In this case the pressure fluctuation in the throat (MG0) is reconstructed using two harmonics like in the signal computed with FLUENT code. At MG1 the pressure fluctuation is rebuilt with four harmonics. The amplitude of the 1st harmonic in MG1 is four times larger than the same amplitude in MG0. However, the 1st harmonic is the most significant like at MG0. The pressure fluctuation at MG2 is reconstructed with twelve harmonics. In this section, the 1st harmonic amplitude still remains most significant at MG2. At MG3 the pressure fluctuation is reconstructed with thirteen harmonics. The amplitude of the first harmonic is the most important while the rest of the harmonics amplitudes are smaller. In this section MG3, the unsteady pressure signals computed with OpenFOAM and FLUENT are significantly different. The vortex rope frequency is 16.3 Hz, corresponding to a Strouhal number of 0.427.

The numerical results are validated against experimental data in order to assess the numerical set-up. Consequently, the Fourier spectra for pressure fluctuations against experimental data are presented in Fig. 6.

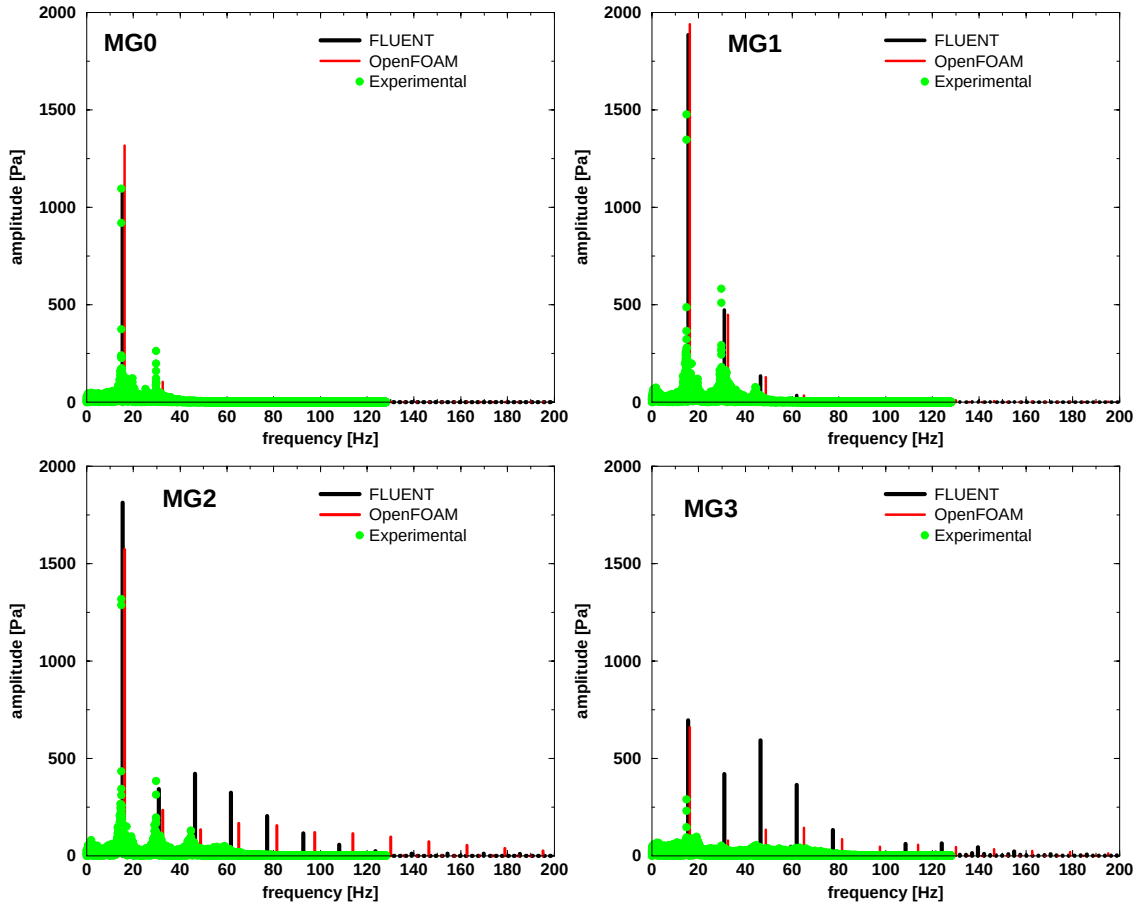

Fig. 6 Frequency spectra from FLUENT (black) and OpenFOAM (red) at locations MG0-3 against experimental data (points).

In MG0, both FLUENT and OpenFOAM codes compute quite well the frequency while the 1st harmonic amplitude is better evaluated by FLUENT. That means, the vortex rope is compact in the throat. In MG1 the Fourier spectra is quite similar for both numerical results. However, the 1st harmonic amplitude is overestimated relative to the experimental data. Consequently, the vortex rope is well developed and more compact in the numerical computation than experimental investigation. In MG2 the amplitude of harmonics computed with FLUENT are quite overestimated than obtained with OpenFOAM. Nevertheless, the

amplitude of 1st harmonic is overestimated by numerical results relative to experimental data. The higher harmonics than 50Hz are not captured due to the upper limit of unsteady pressure transducers. In last section MG3, the numerical signals are significant different from one code to another using k-ε models. Obviously, the vortex rope in the numerical computations using k-ε models is more compact than the experimental investigations.

7. CONCLUSION

The unsteady three-dimensional numerical investigations of the unsteady swirling flow in a conical diffuser with a precessing vortex rope is performed. The precessing vortex rope is computed using k-ε models from FLUENT and OpenFOAM codes. The pressure pulsations computed numerically are compared with experimental data in order to assess the numerical set-up. The fundamental frequency and higher harmonics of the vortex rope is acuratelly captured in the troath as well as resonable evaluated up to middle of the cone. In the last part of the cone the numerical results are significantly different as well as far away from experiment. As a results, the k-ε models reproduce well the unsteady phenomena where the vortex rope is compact. In order to improve the numerical results in the middle and last part of the cone more expansive models will be considered (like LES or DES).

8. ACKNOWLEDGEMENTS

Dr. Sebastian Muntean and Prof. Romeo Susan-Resiga would like to thanks for support to Romanian National Authority for Scientific Research through the CNCSIS PCE 799 project. Dr. Håkan Nilsson is partly financed by SVC (the Swedish Water Power Center, www.svc.nu). SVC has been established by the Swedish Energy Agency, ELFORSK and Svenska Kraftnät together with Chalmers University of Technology, Luleå University of Technology, Uppsala University and the Royal Institute of Technology. Computer resources for the OpenFOAM simulation has been provided by C3SE.

9. REFERENCES

[1] Escudier, M., "Confined Vortices in Flow Machinery", *Ann. Rev. Fluid Mech.*, Vol. 19, 1987, pp. 27- 52.

[2] Dörfler, P., "Mathematical model of the pulsations in Francis turbines caused by the vortex core at part load", *Escher Wyss News*, 1/2, 1980, pp. 101-106.

[3] Cassidy, J.J., and Falvey, H.T., "Observations of unsteady flow arising after vortex breakdown", *J. Fluid Mech.*, Vol. 41, 1970, pp. 727-736.

[4] Nishi, M., Matsunaga, S., Okamoto, M., Uno, M., and Nishitani, K., "Measurement of three-dimensional periodic flow in a conical draft tube at surging condition", *in Rothari, U.S., et al. (eds.), Flows in Non-Rotating Turbo-machinery Components*, FED, Vol. 69, 1988, pp. 81-88.

[5] Susan-Resiga R., Muntean S., Stein P., and Avellan F., "Axi-symmetric Swirling Flow Simulation on the Draft Tube Vortex in Francis Turbines at Partial Discharge" *Proc. 24th IAHR Symposium on Hydraulic Machinery and Systems*, Foz do Iguassu, Brazil, 2008, Paper 13.

[6] Ruprecht A., Grupp J., Al-Salaymeh A., and Kirschner O., "Experimental and Numerical Investigation of Vortex Control in a Simplified Straight Draft Tube Model" Proc. *24th IAHR Symposium on Hydraulic Machinery and Systems*, Foz do Iguassu, Brazil, 2008, Paper 173.

[7] Susan-Resiga, R., Muntean, S., Bosioc, A., Stuparu, A., Milos, T., Baya, A., Bernad, S., and Anton, L.E., "Swirling Flow Apparatus and Test Rig for Flow Control in Hydraulic Turbines Discharge Cone", Proc. *2nd IAHR International Meeting of the Workgroup on Cavitation and Dynamic Problems in Hydraulic Machinery and Systems*, Scientific Bulletin of the "Politehnica" University of Timisoara, Transactions on Mechanics, Tom 52(66), 2007, Fascicola 6, pp. 203-217.

[8] Susan-Resiga R., and Muntean S., "Decelerated Swirling Flow Control in Discharge Cone of Francis Turbine", *Proc. 4th International Symposium on Fluid Machinery and Fluid Engineerin*g, Beijing, China, 2008, pp. 89-96.

[9] Susan-Resiga R., Muntean S., and Bosioc A., "Blade Design for Swirling Flow Generator", *Proc. 4th German-Romanian Workshop on Turbomachinery Hydrodynamics, GROWTH-4*, Stuttgart, Germany, 2008.

[10] Susan-Resiga R., Muntean S., Tanasa C., and Bosioc A., "Hydrodynamic Design and Analysis of a Swirling Flow Generator", *Proc. 4th German-Romanian Workshop on Turbomachinery Hydrodynamics, GROWTH-4*, Stuttgart, Germany, 2008.

[11] Avellan, F., "Flow Investigation in a Francis Draft Tube: The FLINDT Project", *Proc. 20th IAHR Symposium on Hydraulic Machinery and Systems*, Charlotte, USA, 2000, Paper DES-11.

[12] Bosioc A., Susan-Resiga R., and Muntean S., "Design and Manufacturing of a Convergent-Divergent Section for Swirling Flow Apparatus", *Proc. 4th German-Romanian Workshop on Turbomachinery Hydrodynamics, GROWTH-4*, Stuttgart, Germany, 2008.

[13] Muntean, S., Ruprecht, A., Susan-Resiga, R.: A Numerical Investigation of the 3D Swirling Flow in a Pipe with Constant Diameter. Part1: Inviscid Flow Computation. *Scientific Bulletin of the Politehnica University of Timisoara.* 2005.

[14] Fluent Inc., Gambit 2.4 User's Guide, 2006.

[15] Fluent Inc., FLUENT 6.3 User's Guide, 2006.

[16] Visual Numerics, "IMSL Fortran Library User's Guide. Mathematical Functions in Fortran", 2003

[17] Nilsson, H.: Evaluation of OpenFOAM for CFD of turbulent flow in water turbines. Proc. *23rd IAHR Symposium on Hydraulic Machinery and Systems*, Yokohama, Japan, 2006

[18] Nilsson, H., and Gyllenram, W.: Experiences with OpenFOAM for water turbine applications. Proc. 1st OpenFOAM international conference, Old Windsor, United Kingdom, 2007

[19] Nilsson, H., Page, M., Beaudoin, M., Gschaider, B. and Jasak, H.: The OpenFOAM turbomachinery working group, and conclusions from the turbomachinery session of the third OpenFOAM workshop. Proc. 24th *IAHR Symposium on Hydraulic Machinery and Systems*, Foz do Iguassu, Brazil, 2008